Stress effects on the binding energy of shallow-donor impurities in symmetrical GaAs/AlGaAs double quantum-well wires

2007 J. Phys.: Condens. Matter 19 346218

(http://iopscience.iop.org/0953-8984/19/34/346218)

IOP PUBLISHING JOURNAL OF PHYSICS: CONDENSED MATTER

J. Phys.: Condens. Matter **19** (2007) 346218 (13pp) doi:10.1088/0953-8984/19/34/346218

Stress effects on the binding energy of shallow-donor impurities in symmetrical GaAs/AlGaAs double quantum-well wires

Zhan-Guo Bai[1,2] **and Jian-Jun Liu**[1]

[1] College of Physical Science and Information Engineering, Hebei Normal University, Shijiazhuang, Hebei 050016, People's Republic of China
[2] College of Nature, Hebei University of Science and Technology, Shijiazhuang, Hebei 050018, People's Republic of China

E-mail: liujj@mail.hebtu.edu.cn

Received 15 February 2007, in final form 11 June 2007
Published 24 July 2007
Online at stacks.iop.org/JPhysCM/19/346218

Abstract

The effects of applied compressive stress on the binding energies of shallow-donor impurity states with a finite confinement potential in symmetrical GaAs/AlGaAs double quantum-well wires (DQWWs) are studied theoretically using a variational procedure within the effective-mass approximation. Significant results for different wire and barrier widths, shallow-donor impurity positions, and compressive stress along the growth direction of the structure are obtained taking into account the Γ–X crossover and the image charge effects in the calculations. Our results show that the binding energy does not change appreciably with the size of the wire and barrier, or with the donor ion position. We also find that for stress values up to 13.5 kbar, the binding energy increases linearly with stress, while for stress values greater than 13.5 kbar, the binding energies show nonlinear behavior. Moreover, in the limit of double quantum wells (DQWs), our binding energy agrees with previously reported results. It is pointed out that compressive stress is an important factor in studies of the binding energies of shallow-donor impurity states in symmetrical GaAs/AlGaAs DQWWs.

1. Introduction

In recent years, based on the rapid progress in experimental crystal-growth techniques, such as metal-organic chemical-vapor deposition, liquid-phase epitaxy, and molecular-beam epitaxy, the external stress effects on impurity states of low-dimensional systems have received increased attention both theoretically and technologically. These new crystal-growth techniques open up opportunities to study the optoelectronic properties and band structure of semiconductor superlattices and heterostructures under hydrostatic pressure, including

coupling effects, resonant tunneling effects, and polarizability phenomena. It is now known that these effects can be enhanced under hydrostatic pressure, a fact which may lead to many potential applications in optoelectronic devices [1–6], such as strained semiconductor quantum-well lasers, transducers, infrared detectors, resonant tunneling diodes, and ballistic transistors.

Many experimental and theoretical investigations have been reported concerning the effects of hydrostatic pressure and compressive stress on shallow-donor impurity states in GaAs/$Al_xGa_{1-x}As$ quantum wells (QWs) and quantum-well wires (QWWs). Gonzalez *et al* [7] studied the optical properties related to pressure in QWWs, and Odhiambo [8] reported a comparative study of hydrostatic pressure in single quantum wells (SQWs) and double quantum wells (DQWs). The Γ–X crossover [9, 10] was observed experimentally by Venkateswaran *et al*, who studied the pressure dependence of photoluminescence spectra in multiple quantum-well (MQW) structures. Elabsy *et al* [11–17] calculated the effects of compressive stress on the binding energies of shallow-donor impurity states in SQWs. These results show that, for a given SQW thickness, the binding energy increases with increasing pressure. Recently, Schweizer *et al* [18] reported that a rectangular-section GaAs/AlGaAs single quantum-well wire (SQWW) structure down to 40 nm and quantum-dot structures of 100 nm radius can be constructed successfully with the masked implantation-enhanced intermixing technique. In [19–24], the effects of resonant tunneling and coupling between quantum wells under hydrostatic pressure or uniaxial stress were investigated in DQWs and in double-barrier MQW structures. In addition, some authors [25–33] have calculated the density of states and polarizability of shallow-donor impurities. They have found that the density of states and polarizability strongly depend on the external stress. Theoretical studies of the Γ–X crossover effect on the binding energies of the impurity states in SQWs have been reported by Elabsy [34–36], who obtained the stress dependence in low-dimensional systems of various parameters such as the well widths, effective masses, dielectric constants, and barrier heights. As a general feature, the binding energies of the impurity states increase with increasing pressure and decreasing size of the structures.

Recently, there has been an increasing interest in understanding stress effects in low-dimensional semiconductor structures, which have been predicted to have a wealth of fascinating new properties [12–15]. For example, a uniaxial stress effect can lead to strong anisotropy in the subband dispersion and the Fermi surface in p-type heterostructures [12]. For a given structure, the energy difference between type-I and type-II transitions can be tuned with hydrostatic pressure in a continuous and reversible manner, which makes it possible to understand the mechanisms of various interband transitions [13]. Desrat and Maude observed the carrier density in symmetrical GaAs/AlGaAs QWs which can be tuned by application of hydrostatic pressure and illumination [14]. The effects of compressive stress on the binding energies and the density of shallow-donor impurity states in symmetrical GaAs/AlGaAs DQWs was studied by Raigoza *et al*. They found that, for various widths of the well and barrier, the binding energy shows a linearly behavior in the low-pressure regime and nonlinear behavior under high-pressure due to the Γ–X crossing effect [37]. In fact, the double quantum-well wire (DQWW) structure is more significant due to stronger confinement and acts as a bridge between the SQWW and superlattices. Consequently the stress effects on the binding energies of shallow-donor impurities in DQWWs structures are very important, but they have not yet been studied as far as we are aware.

In the present work, using the variational method and the effective-mass approximation, we conduct a theoretical study of the effects of an external compressive stress on the binding energies of shallow-donor states in symmetrical GaAs/$Al_xGa_{1-x}As$ DQWW structures. The mismatch effects of the effective electron mass in the wire and barrier material and the Γ–X crossing effect are taken into account in calculation. The paper is organized as follows.

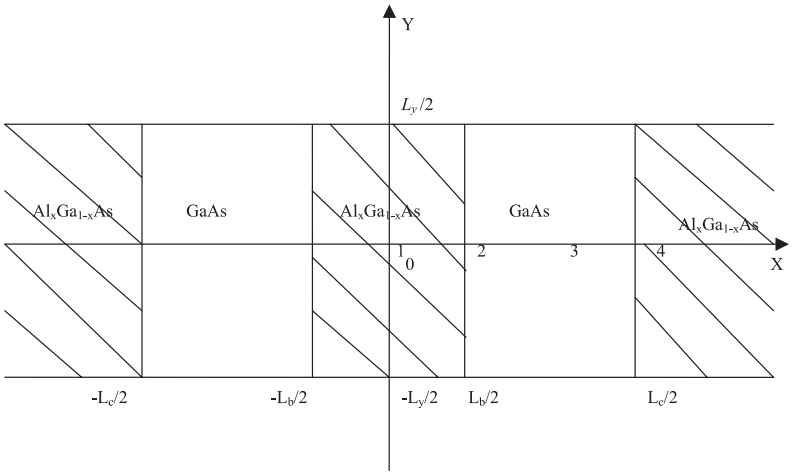

Figure 1. The rectangular cross section of the symmetrical GaAs/$Ga_{1-x}Al_xAs$ DQWWs; the labels 1, 2, 3, and 4 correspond to the donor ion located at the barrier center, barrier edge, wire center, and wire edge, respectively.

In section 2 we present our theoretical model. Our results and discussion are presented in section 3, and finally, in section 4, the conclusions obtained are summarized briefly.

2. Theoretical model

A symmetrical DQWW structure is sketched in figure 1. The origin of the coordinate system is chosen at the center of the center barrier, and the movement of electrons is confined in the x and y directions while it is free along the z axis. Taking into account the effects of the temperature (T) and of a compressive stress (P), the Hamiltonian for a shallow-donor impurity including image potential in the GaAs/$Al_xGa_{1-x}As$ DQWW in the x direction has the following form:

$$H = -\frac{\hbar^2}{2m^*_{w,b}(P,T)}\nabla^2 - \frac{e^2}{\varepsilon_{w,b}(P,T)r} + V(x,y,P,T) + V_{im}(r), \tag{1}$$

where $r = [(x-x_i)^2 + (y-y_i)^2 + z^2]^{1/2}$ is the distance between the electron and the donor ion.

The donor ion position along the growth axis (x direction) is denoted by $\vec{r}_i = (x_i, y_i, 0)$. The parameters $m^*_{w,b}(P,T)$ and $\varepsilon_{w,b}(P,T)$ are the parabolic conduction effective mass and the stress-dependent GaAs static dielectric constant, respectively. The subscripts w and b denote the wire and the barrier layer materials, respectively [37]. The potential $V(x,y,P,T)$ confining the electron in the DQWWs in equation (1) is given by

$$V(x,y,P,T) = \begin{cases} V_0(P,T), & |x| \geqslant L_c, \quad |x| \leqslant \frac{L_b}{2}, \quad |y| < \frac{L_y}{2}, \\ 0, & \frac{L_b}{2} < |x| < L_c, \quad |y| < \frac{L_y}{2}, \\ \infty, & |y| \geqslant \frac{L_y}{2}, \end{cases} \tag{2}$$

where $V_0(P,T)$ is the stress-dependent barrier height [37], L_w and L_y are, respectively, the dimensions of the quantum wire in the x and y directions; L_x or L_b is width of the central barrier layer. We also use $L_c = L_b/2 + L_w$, $L_b = L_x$, where $L_w(0)$ and $L_b(0)$ denote the values at zero stress [12, 38–40]. For nonzero stress,

$$L_{w,b}(P) = L_{w,b}(0)[1 - (S_{11} + 2S_{12})P], \tag{3}$$

where $S_{11} = 11.6 \times 10^{-3}$ kbar^{-1}, and $S_{12} = -3.7 \times 10^{-4}$ kbar^{-1} are the elastic constants of GaAs [24, 34]. The donor ion image potential can be written as [40]

$$V_{\text{im}}(r) = -2 \sum_{n_x,n_y=0}^{\infty} \sum_{j_1,j_2} \left(\frac{\varepsilon_{\text{w}} - \varepsilon_{\text{b}}}{\varepsilon_{\text{w}} + \varepsilon_{\text{b}}}\right)^{n_x+n_y} \left[(x - x_i^{j_1}(n_x))^2 + (y - y_i^{j_2}(n_y))^2 + z^2\right]^{-1/2}$$
$$(j_1, j_2 = +, -),$$

which can be treated as a perturbation for the small influence on binding energy. Following [13, 20, 32, 37, 41], the trial wavefunction for the ground state can be chosen to be

$$\psi(r) = Nf(x, y)g(r), \tag{4}$$

where N is a normalization constant, $g(r) = \exp(-\lambda r)$ is the hydrogenic part, λ is the variational parameter, and $f(x, y)$ is the eigenfunction of the Hamiltonian in equation (1) without the impurity potential term. In the region $|y| \geqslant L_y/2$, $f(x, y) = 0$, and in the region $|y| < L_y/2$, $f(x, y)$ is given by

$$f(x, y) = f(y)f(x) = \cos\left(\frac{\pi y}{L_y}\right) \begin{cases} A\mathrm{e}^{k_{2x}(x+L_{\text{c}})}, & x \leqslant -L_{\text{c}}, \\ -B\sin\left[k_{1x}\left(x + \dfrac{L_{\text{b}}}{2}\right)\right] + C\cos\left[k_{1x}\left(x + \dfrac{L_{\text{b}}}{2}\right)\right], & \\ \quad -L_{\text{c}} < x < -\dfrac{L_{\text{b}}}{2}, & \\ \dfrac{1}{2}(\mathrm{e}^{k_{2x}x} + \mathrm{e}^{-k_{2x}x}), & |x| \leqslant \dfrac{L_{\text{b}}}{2}, \\ B\sin\left[k_{1x}\left(x - \dfrac{L_{\text{b}}}{2}\right)\right] + C\cos\left[k_{1x}\left(x - \dfrac{L_{\text{b}}}{2}\right)\right], & \\ \quad \dfrac{L_{\text{b}}}{2} < x < L_{\text{c}}, & \\ A\mathrm{e}^{-k_{2x}(x+L_{\text{c}})}, & x \geqslant L_{\text{c}}, \end{cases} \tag{5}$$

where the coefficients A, B, and C can be obtained from the matching conditions for the eigenfunctions at the interface. The corresponding eigenvalue $E_0^x(P, T)$ associated with $f(x)$ can be obtained as the first root of the transcendental equation

$$2\cos(k_{1x}L_{\text{w}}) + \left(\beta - \frac{1}{\beta}\right)\sin(k_{1x}L_{\text{w}}) - \left(\beta + \frac{1}{\beta}\right)\sin(k_{1x}L_{\text{w}})\mathrm{e}^{-k_{2x}L_{\text{b}}} = 0, \tag{6}$$

where

$$\beta = \frac{m_{\text{w}}^* k_{2x}}{m_{\text{b}}^* k_{1x}}, \qquad k_{1x} = \left[\frac{2m_{\text{w}}^*(P, T)}{\hbar^2} E_0^x(P, T)\right]^{1/2},$$
$$k_{2x} = \left[\frac{2m_{\text{b}}^*(P, T)}{\hbar^2}(V_0(P, T) - E_0^x(P, T))\right]^{1/2},$$

and the eigenvalue $E_0^y(P, T) = (\pi/L_y)^2$. The binding energy including the compressive stress is given by

$$E_{\text{b}}(P, T) = E_0(P, T) - E_{\text{min}}(P, T), \tag{7}$$

where $E_{\text{min}}(P, T)$ is the eigenvalue with the impurity potential term taken into account, and is minimized with respect to the variational parameter λ. $E_0(P, T)$ is the ground-state eigenvalue of the Hamiltonian in equation (1) without the impurity potential term, $E_0(P, T) = E_0^x(P, T) + E_0^y(P, T)$.

In the following calculations we use $x = 0.3$, and the impurity image potential only up to second-order terms. Our attention is mainly focused on the stress effects, and our results for a symmetrical GaAs/$Ga_{1-x}Al_x$As DQWW are presented at $T = 4$ K.

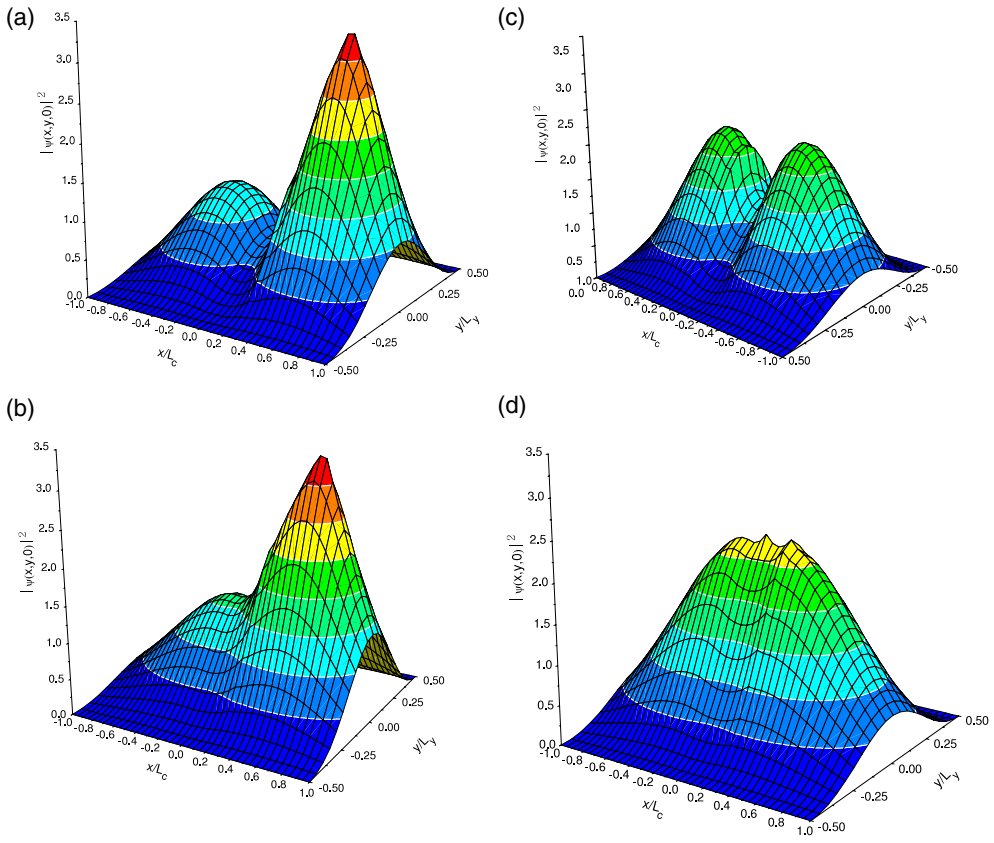

Figure 2. Probability density of an electron in symmetrical GaAs/$Ga_{1-x}Al_xAs$ DQWWs with $L_w = 50$ Å, $L_b = 20$ Å, $L_y = 100$ Å, for $P = 10$ kbar ((a), (c)) and $P = 30$ kbar ((b), (d)). Figures (a) and (b) are for a donor ion located at the center of the right wire, and figures (c) and (d) are for a donor ion located at the center of the barrier.

(This figure is in colour only in the electronic version)

3. Results and discussion

First, we show the probability density of an electron in symmetrical GaAs/GaAlAs DQWWs with $L_w = 50$ Å and $L_b = 20$ Å. Figure 2 shows results for the donor ion located at two positions and for two given values of the external stress. From figure 2, it can be seen that the probability density depends strongly on compressive stress. With increasing applied stress for the two donor ion positions, the coupling effect between the two quantum wires becomes strong. When the donor ion is located at the center of the right wire (figures 2(a) and (b)), the probability density shows an asymmetric distribution. The maximum value of the probability density occurs at the center of the right wire for the two stress values, and the minimum value occurs at the center of the barrier. The second maximum value is located at the center of the left wire. Comparing figures 2(a) and (b), it can be seen that more of the wavefunction can penetrate to the left wire with increasing pressure due to the reduction in the barrier height, which leads to a larger probability density of the electron in the region of the left wire and a stronger coupling effect. However, as shown in figures 2(c) and (d), the probability density exhibits a symmetric distribution for the two values of the applied stress when the donor ion is located at the barrier

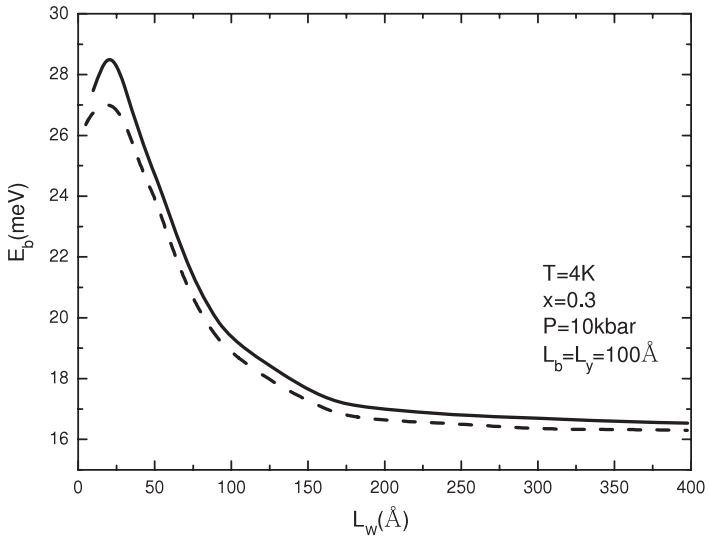

Figure 3. Binding energy of a donor impurity as a function of wire widths for both image potential (solid lines) and neglecting the effect of image charge (dashed lines) in symmetrical GaAs/$Ga_{1-x}Al_xAs$ DQWWs with $L_b = L_y = 100$ Å and for $P = 10$ kbar.

center. The absolute maximum of the probability density occurs at the center of each wire for $P = 10$ kbar. While $P = 30$ kbar, our result agrees with the result given in [37]. The reason is that the lower barrier height weakens the potential barrier, impeding the wavefunction, and the Coulomb interaction becomes stronger. The electron therefore has a greater probability to be distributed into the barrier center.

In figure 3, the binding energies of a donor impurity including the image charge are compared with those without image potential as a function of the wire width. It can be seen that the binding energy increases due to the effects of the image charge, and the difference in binding energies between the results of two cases decreases with increasing wire size, which is in agreement with the results of [40]. Furthermore, we find that the two curves have same variation tendency with the wire width; that is to say, the charge image effects do not affect the variation behavior of the binding energy. This study mainly focused on the stress effects on impurity states. So the charge image effects are not included in following figures. Of course, strictly speaking, the image potential in quantum wires cannot be neglected in considering electronic and impurity states, especially when the dimensions of the wires are small [42].

The influence of an applied compressive stress on the binding energy of a donor impurity is shown in figure 4 for different positions of the donor ion. Two DQWW structures are considered. From figure 4 we can see that the binding energy increases slowly with increasing compressive stress for the low-pressure direct gap regime (stress values up to 13.5 kbar). It shows linear behavior in the direct gap regime because the barrier height remains constant up to 13.5 kbar. Small variations in wire widths, and effective mass with pressure cannot appreciably affect the binding energy. For high pressure (stress values larger than 13.5 kbar), the binding energy shows a nonlinear variation with increasing external stress where semiconductor structures turn into the indirect regime due to the Γ–X crossing effects. The two curves labelled 3 in figure 4 show that the binding energy first increases with increasing external stress until it reaches a peak value and then diminishes as a result of the effects of the electron effective masses, the dielectric constant, and the barrier height. It is very interesting that the binding

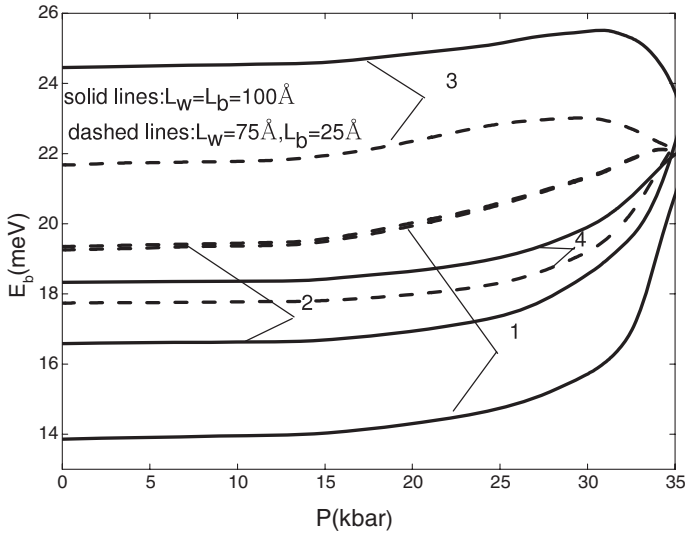

Figure 4. Binding energy of a donor impurity as a function of the compressive stress in symmetrical GaAs/$Ga_{1-x}Al_xAs$ DQWWs with $L_w = L_b = 100$ Å, $L_y = 100$ Å (solid lines) and $L_w = 75$ Å, $L_b = 25$ Å, $L_y = 100$ Å (dashed lines). The labels 1, 2, 3, and 4 are the same as those in figure 1.

energy for two stress values can be the same value. It should be noted in figure 4 that the binding energy in the solid curve 3 is higher than those of the dashed ones. This phenomenon can be understood because the binding energy shows similar behavior to that of a single quantum wire due to the weak coupling effects when the barrier width is large. It should also be noted that the coupling of the two wires becomes strong as the barrier width decreases, thus diminishing the binding energy. For curves 1, 2, and 4, the binding energy is lower than that of curve 3, due to the repulsion of the wavefunction by the potential barrier when the donor ion is at edge of the barrier or the two walls of the wire, thus leading to a large distance between the electron and donor ion. In addition, we obtained results for the binding energy in the limiting case $L_y = 3000$ Å, in which the DQWW turns into a DQW, as shown in figures 5(a) and (b). In figure 5(a) the barrier width is $L_b = 500$ Å when the structure turns into two uncoupled SQWs, as can be seen in figure 8. It is $L_b = 25$ Å in figure 5(b) in which DQWWs turn into a coupled DQW. Consequently, our results are lower than those of [34] and higher than those of [37], as expected. Our calculation confirms previous results for a SQW [34] and DQW [37].

In figure 6 we plot the binding energy of a donor impurity as a function of the position of the donor ion in the growth direction in symmetrical GaAs/$Ga_{1-x}Al_xAs$ DQWWs and for different values of the external compressive stress. The sizes of the two structures are taken to be $L_w = L_b = 50$ Å (solid lines) and $L_w = 50$ Å, $L_b = 100$ Å (dashed lines). From figure 6 it can be seen that the binding energy has a minimum value when the donor ion is located at the center of the barrier, and that the binding energy first increases as the donor ion moves from the center of the barrier to the edge of the right wire. It can also be seen that the binding energy increases with external pressure. The maximum value of the binding energy occurs when the donor ion lies close to the center of the wires. The binding energy then diminishes when the donor ion approaches the edge of the wire. This is because when the donor ion is located near the center of the wire, the electron cloud has more opportunity to be close to the donor ion, which means strong confinement. However, on average the electron is farther from the donor

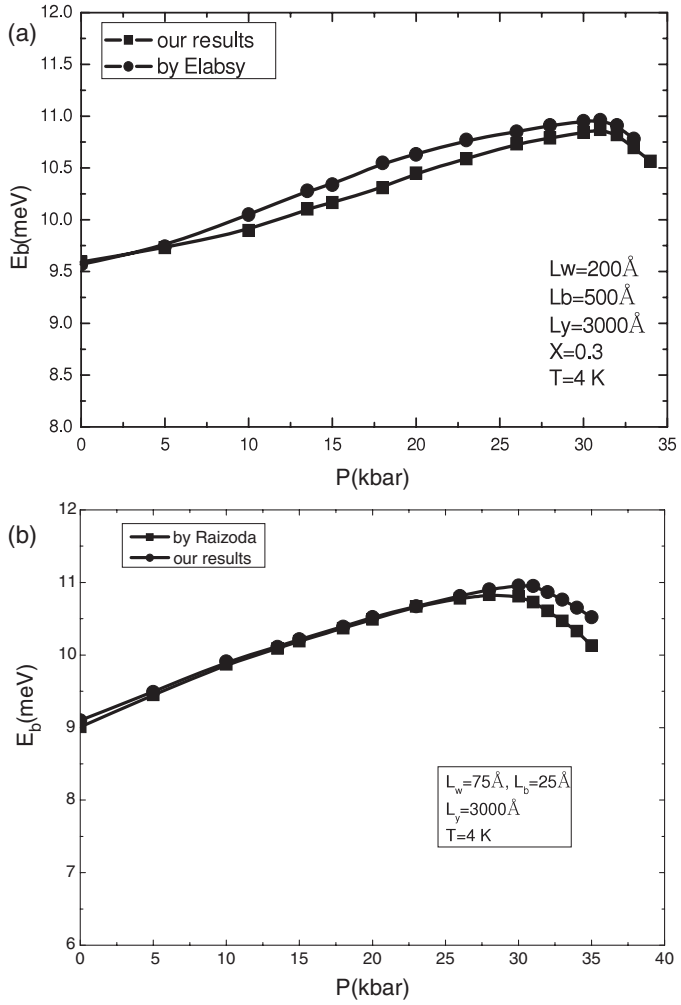

Figure 5. (a) Binding energy of a donor impurity as a function of the compressive stress in symmetrical GaAs/$Ga_{1-x}Al_xAs$ DQWWs. The sizes of the structures are $L_w = 200$ Å, $L_b = 500$ Å, with the limit condition of $L_y = 3000$ Å (donor ion position located at the center of the wire). (b) Binding energy of a donor impurity as a function of the compressive stress in symmetrical GaAs/$Ga_{1-x}Al_xAs$ DQWWs. The sizes of the structures are $L_w = 75$ Å, $L_b = 25$ Å, with the limit condition of $L_y = 3000$ Å (donor ion position located at the center of the wire).

ion when the donor ion position is close to the center of the barrier, which means that the large distance between the electron and donor ion weakens the Coulomb interaction, thus reducing the binding energy. For a given pressure, the binding energy increases with decreasing barrier width for various donor ion positions except the center of the wire, due to the small structure sizes, which is equivalent to a large confinement. However, we also see that the binding energy diminishes in the wire regime owing to the small barrier width, which strengthens the coupling of the two wires as a result of the increased wavefunction penetration (see figure 2(b)). In addition, when the donor ion is in the wire region there is a crossing between two solid lines, which shows that the binding energy for two stress values can have the same value as discussed in figure 4. Moreover, there are also crossings between the dashed lines and all of the solid

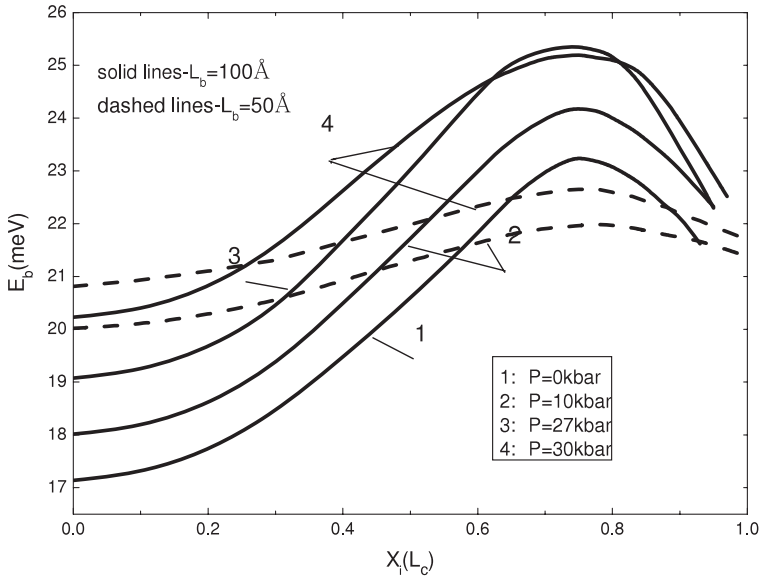

Figure 6. Binding energy of a donor impurity as a function of the position of the donor ion in the growth direction in symmetrical GaAs/$Ga_{1-x}Al_xAs$ DQWWs. The solid lines denote the results for $L_w = 50$ Å, $L_b = 100$ Å, $L_y = 100$ Å, and the dashed lines denote the results for $L_w = 50$ Å, $L_b = 50$ Å, $L_y = 100$ Å. The labels 1, 2, 3, 4 correspond to $P = 0$, 10, 27 and 30 kbar, respectively.

ones in figure 6. This means that the binding energy of the two structures can have the same values. These crossing are very important and useful in device applications.

Figure 7 gives the binding energy of a donor impurity as a function of the wire width for the two different values of the external compressive stress. The labels 1, 2, 3, and 4 are the same as those in figure 1. In figure 7(a), the overall behavior of the curves is similar to that in symmetric GaAs/GaAlAs DQWs [37]. However, our values are larger than those in [37] due to the reduction of the dimensionality of our structures. As shown in figure 7(a), the binding energy increases with wire widths up to a maximum value and then decreases with increasing width of the wire for all four donor ion positions and for both values of the compressive stress. Because the quantum confinement effect dominates the binding energy in wires of small widths, the Coulomb interaction is weakened with increasing wire width, and the distance between the electron and the donor ion becomes larger as a result of the decreased binding energy. We also observe that, for small wire widths, the variation in the binding energy caused by the donor ion positions is small. Additionally, for the donor ion positions in the wires, the binding energy decreases more quickly than that of [37] due to the fact that the coupling between the two wires for the $L_b = 100$ Å case is stronger than that for $L_b = 200$ Å [37]. It is also worth noting that the binding energy approaches a limit when the wire widths become sufficiently large and that the limit is equal to the value for bulk GaAs. The mean value of the distances between the donor ion and the electron as a function of wire width is shown in figure 7(b). The opposite variational tendency of the curves for the binding energy and the mean values of distances in figure 7(b) is expected from the above discussion. It is important to point out that for various donor ion positions except in the wires, the dashed curves (corresponding to 30 kbar) are higher than the solid ones (10 kbar), which shows that the binding energy increases with applied stress in agreement with the discussion of figure 4. When the donor ion is located at the center of the wire, the binding energies' compressive stress at $P = 30$ kbar are lower than those in the

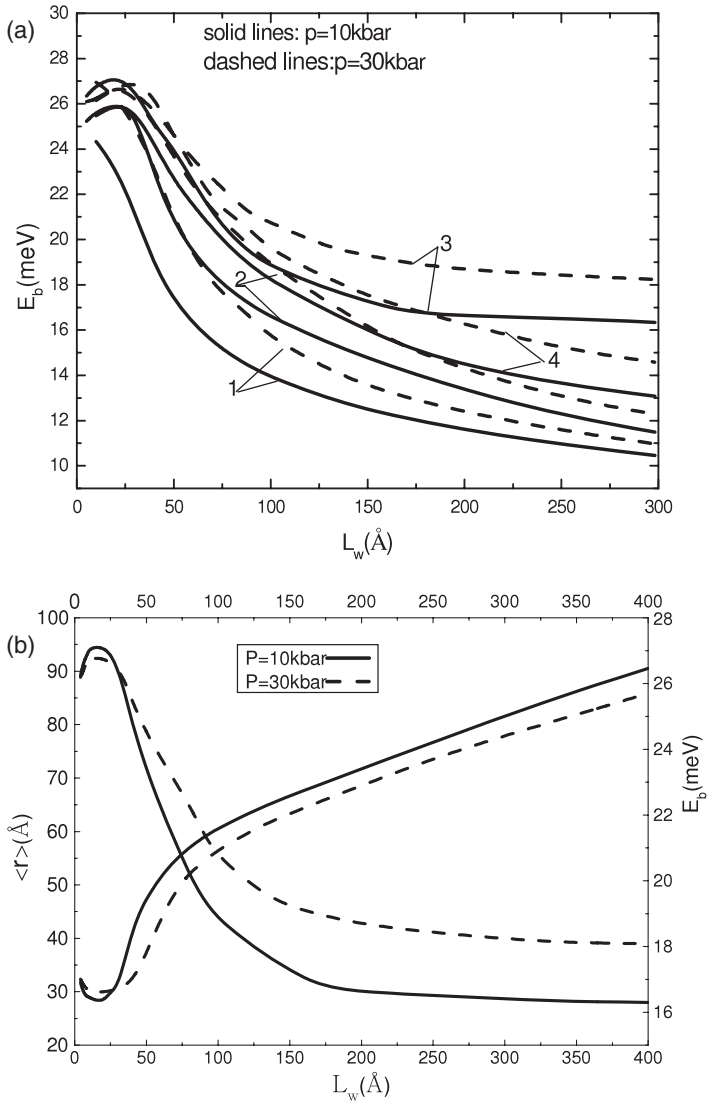

Figure 7. (a) Binding energy of a donor impurity as a function of the wire width in symmetric GaAs/$Ga_{1-x}Al_xAs$ DQWWs with $L_b = L_y = 100$ Å and for $P = 10$ kbar (solid lines), $P = 30$ kbar (dashed lines). The labels 1, 2, 3, and 4 are the same as those in figure 1. (b) Binding energy and the average values of distances between the donor ion and the electron as a function of wire width when the donor ion is located at the center of the wire.

$P = 10$ kbar case in small wire widths, which can be understood when the kinetic energy of the electron is great and the barrier height decreases with compressive stress, with the result that the electron can easily penetrate the potential barrier into the left wire, and as a result the binding energies decrease.

Finally, figure 8 shows the binding energy of a donor impurity as a function of the central barrier width in symmetric GaAs/GaAlAs DQWWs for the two cases $L_w = 100$ Å, $P = 10$ kbar (solid lines), and $L_w = 100$ Å, $P = 30$ kbar (dashed lines). The labels 1, 2, 3, and 4 are the same as those in figure 1. The different curves for the different positions of the

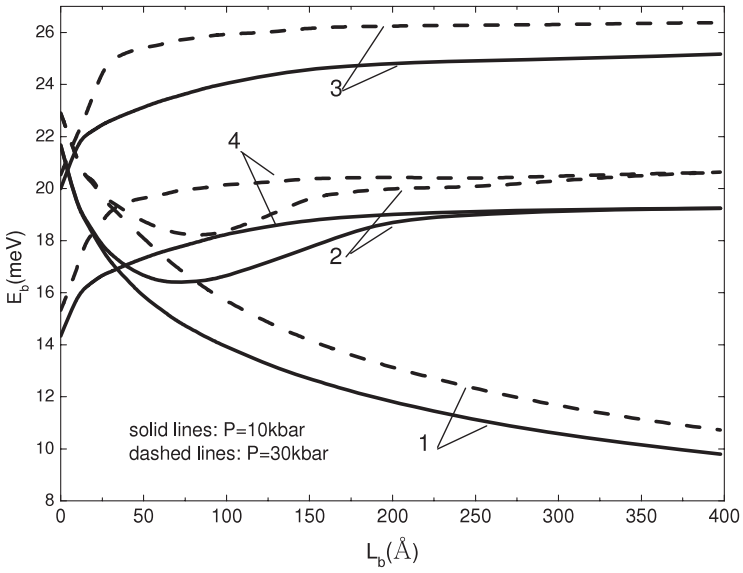

Figure 8. Binding energy of a donor impurity as a function of the central barrier width in symmetrical GaAs/$Ga_{1-x}Al_xAs$ DQWWs with $L_w = 100$ Å, $L_y = 100$ Å. The solid lines denote the result for $P = 10$ kbar and the dashed lines denote the result for $P = 30$ kbar. The labels 1, 2, 3, and 4 are the same as those in figure 1.

donor ion show different variational behavior as a function of barrier width: when the donor ion located at the center of the barrier, the binding energy diminishes with increasing central barrier width and goes to the value of bulk GaAlAs materials in the limit as L_b goes to infinite for both values of the external compressive stress. The reason is that the corresponding value of the distance between the electron and the donor ion goes to infinity and the Coulomb interaction goes to zero. For the curves 2, in the $L_b = 0$ limit, the same behavior is seen as with the curves labelled 1, initially due to the wavefunction extending itself in a SQWW of 200 Å width [13]. With a nonzero barrier, the wavefunction spatial symmetry is broken, which increases the expectation value of the distance between the electron and the donor ion, and the binding energy decreases as a result of the weakness of Coulomb interaction. When L_b increases, the left wire becomes gradually decoupled as a result of the increasing binding energy. For large barrier widths, the binding energy manifests a more uniform behavior compared with the previous cases. This uniform behavior shows that the effect of pressure is very small when the barrier width is large. Curves 3 and 4 show similar results: for small central barrier widths the binding energy increases with increasing barrier width until the central barrier becomes sufficiently large, after which the binding energy remains almost constant due to the uncoupling of adjacent wires. This case is similar with those in [37], but our values are larger than those of [37] due to the fact that the reduction in dimensionality increases the confinement, as discussed before. It is also seen that the binding energies always increase with increasing external pressure for various donor ion positions, which emphasizes the very important role of the applied compressive stress in determining the binding energy.

4. Conclusion

By means of a variational procedure within the effective-mass approximation we have investigated the effect of compressive stress on the binding energies of shallow-donor impurity

states in symmetrical GaAs/AlGaAs DQWWs with finite potential barrier height. The stress was applied in the x direction (the growth direction of the structure) and the donor ion is located at various positions along the x axis. Taking into account the pressure-related crossover and image potential we have investigated the effect of different values of the compressive stress, different widths of the wire and barrier and various positions of the donor ion. As a general feature, we observe that, for various positions of the donor ion, the coupling effects become strong when the barrier widths become small for fixed applied stress. On the other hand there is increasingly strong coupling with increasing applied stress for the same barrier widths. This can be seen from the probability density for the two values of the applied stress (figure 2). Our results show that the binding energy increases linearly with applied stress for various dimensions of the wires and barrier, and for values of compressive stress up to 13.5 kbar. When the applied compressive stress values are larger than 13.5 kbar, the binding energy increases to a peak value, and then decreases when the donor ion is located in the quantum wire regime (figure 4). The binding energies show nonlinear behavior as a function of stress due to the decrease of the barrier height, which is related to the external pressure. The binding energy for the limiting cases in which a DQWW turns into a DQW is reported as well. It should be noted that the binding energy increases with decreasing L_b, and there is a crossing for different values of the barrier width in the well region in which two structures of different dimensions can be tuned to the same energy. This is important in real device applications. The discussions above confirm that compressive stress plays a very important role in the study of the binding energy of shallow-donor impurity states in symmetrical GaAs/AlGaAs DQWWs.

Acknowledgments

This work was supported by the National Natural Science Foundation of the People's Republic of China under Grant No. 10674040 and the Science and Technology Innovation Foundation of Hebei province under Grant Nos 06547006D and A2007000233.

References

[1] Adachi S 1985 *J. Appl. Phys.* **58** R1
[2] Smith J M, Klipstein P C, Grey R and Hill G 1998 *Phys. Rev.* B **57** 1740
[3] Dai N, Huang D, Liu X Q, Mu Y M, Lu W and Shen S C 1998 *Phys. Rev.* B **57** 6566
[4] Adrian C, Sahu B R and Leonard K 2006 *Phys. Rev.* B **73** 214105
[5] Endicott J, Patane A, Maude D, Eaves L, Hopkinson M and Hill G 2005 *Phys. Rev.* B **72** 041306(R)
[6] Barati M, Vahdani M R K and Rezaei G 2007 *J. Phys.: Condens. Matter* **19** 136208
[7] Conzalez J W, Lopez S Y, Rodriguez A H, Porras-Montengro N and Duque C A 2007 *Phys. Status Solidi* b **244** 70
[8] Odhiambo O H, Porras-Montengro N, Lopez S Y and Duque C A 2007 *Phys. Status Solidi* c **4** 298
[9] Venkateswaran U, Chandrasekhar M, Chandrasekhar H R, Wolfram T, Fischer R, Masselink W T and Morkoc H 1985 *Phys. Rev.* B **31** 4106
[10] Burnett J H, Cheong H M, Paul W, Koteles E S and Elman B 1993 *Phys. Rev.* B **47** 1991
[11] Elabsy A M 1993 *Phys. Scr.* **48** 376
Chang Y C and Jimes R B 1989 *Phys. Rev.* B **39** 12672
[12] Kolokolov K I, Beneslavski S D, Minina N Ya and Savin A M 2001 *Phys. Rev.* B **63** 195308
[13] Morales A L, Montes A, Lopez S Y and Duque C A 2002 *J. Phys.: Condens. Matter* **14** 987
[14] Raigoza N, Duque C A, Reyes-Gorez E and Oliveira L E 2006 *Phys. Status Solidi* b **243** 635
[15] Liu J-J, Shen M and Wang S-W 2007 *J. Appl. Phys.* **101** 073703
[16] Tessema G and Vianden R 2005 *Appl. Surf. Sci.* **240** 146
[17] Lopez S Y, Porras-Montengro N and Duque C A 2005 *Physica* B **362** 41
[18] Schweizer H, Lehr G, Prins F, Mayer G, Lach E, Kuger R, Frohlich E, Pilkuhn M H and Smith G W 1992 *Superlatt. Microstruct.* **12** 419

[19] Desrat W, Maude D K, Wasilewski Z R, Airey R and Hill G 2006 *Phys. Rev.* B **74** 193317
[20] Chen H and Zhou S 1987 *Phys. Rev.* B **36** 9581
[21] Chaudhuri S 1983 *Phys. Rev.* B **28** 4480
[22] Smith J M, Klipstein P C, Grey R and Hill G 1998 *Phys. Rev.* B **57** 1746
[23] Gil B, Lefebvre P, Bonnel P, Mathieu H, Deparis C, Massies J, Neu G and Chen Y 1993 *Phys. Rev.* B **47** 1954
[24] Morales A, Montes A, Lopez S Y, Raigoza N and Duque C A 2003 *Phys. Status Solidi* c **0** 652
[25] Aspnes D E 1976 *Phys. Rev.* B **14** 5331
[26] Wolford D J and Bradley J A 1985 *Solid State Commun.* **53** 1069
[27] Thien Cao H and Tran Thoai D B 1996 *Solid State Commun.* **97** 643
[28] Burnett J H, Cheong H M, Paul W, Koteles E S and Elman B 1993 *Phys. Rev.* B **47** 1991
[29] Chandrasekhar M and Chandrasekhar H R 1994 *Phil. Mag.* B **70** 369
[30] Oyoko H O, Duque C A and Porras-Montenegro N 1994 *J. Appl. Phys.* **90** 579
[31] Elabsy A M 1993 *Phys. Scr.* **48** 376
[32] Lopez S Y, Porras-Montenegro N and Duque C A 2003 *Phys. Status Solidi* c **0** 648
[33] Stehr D, Helm M, Metzner C and Wanke M C 2006 *Phys. Rev.* B **74** 085311
[34] Elabsy A M 1994 *J. Phys.: Condens. Matter* **6** 10025
[35] Duque C A, Morales A L, Montes A and Porras-Montenegro N 1997 *Phys. Rev.* B **55** 10721
[36] Elabsy A M 1993 *Superlatt. Microstruct.* **14** 65
[37] Raigoza N, Morales A L, Montes A, Porras-Montenegro N and Duque C A 2004 *Phys. Rev.* B **69** 045323
[38] Oyoko H O, Duque C A and Porras-Montenegro N 2001 *J. Appl. Phys.* **90** 819
[39] Samara G A 1983 *Phys. Rev.* B **27** 3494
[40] Elabsy A M 1992 *Phys. Rev.* B **46** 2621
Deng Z Y, Lai T R and Guo J K 1994 *Phys. Rev.* B **50** 5732
[41] Yu P Y and Cardona M 1998 *Fundamentals of Semiconductors* (Berlin: Springer)
[42] Deng Z Y, Lai T R, Guo J K and Gu S W 1994 *J. Appl. Phys.* **75** 7389